ELSEVIER

Journal of Volcanology and Geothermal Research 69 (1995) 197–215

Journal of volcanology and geothermal research

Eruption of a major Holocene pyroclastic flow at Citlaltépetl volcano (Pico de Orizaba), México, 8.5–9.0 ka

Gerardo Carrasco-Núñez [a,b,*], William I. Rose [a]

[a] *Department of Geological Engineering, Geology, and Geophysics Michigan Technological University Houghton, MI 4993, USA*

[b] *Departamento de Geologia Regional Instituto de Geología, U.N.A.M. Cd. Universitaria, Coyoacán 04510, México D.F, Mexico*

Received 22 August 1994; accepted 13 February 1995

Abstract

Multiple volcanic eruptions occurred between 8500 and 9000 yr. B.P. from the central crater of Citlaltépetl Volcano generating a series of pyroclastic flows that formed a deposit with a total volume of about 0.26 km^3 (D.R.E.). The flows descended in all directions around the crater, but they were mostly controlled by topography and deposited in valleys or local topographic depressions up to about 30 km from vent. Although the flows were apparently emplaced without much violence, some features of the deposits reveal local turbulent conditions and an expanded fluidization that can be related to moderate flow velocities. The deposit has two members: the lower one consists of multiple flow units, and the upper one includes a single flow unit and a thin basal pumice-fall. Both members are lithologically similar and dominated by dense, andesitic scoriae with minor amounts of different pumice types (andesitic, dacitic, and banded), and lithics in a silty matrix.

The eruption probably had a low-pressure 'boiling-over' mechanism and was possibly triggered by mixing of dacitic and andesitic magmas. Juvenile material in the pyroclastic-flow deposit is compositionally similar to that of Holocene lava flows at Citlaltépetl, which have apparently resulted from magma homogenization of mafic and silicic end members. Because the system is continuously injected with new basaltic-andesitic magma, a recurrence of explosive activity is possible in future eruptions.

1. Introduction

Citlaltépetl (Pico de Orizaba) is the easternmost active volcano of the Mexican Volcanic Belt (Fig. 1), forming the southern end, along with Sierra Negra volcano, of a nearly north–south trending volcanic chain composed of deeply eroded calderas and an extinct stratovolcano. Ice-capped Citlaltépetl is built of andesitic and dacitic lavas that form a symmetrical stratovolcano with a truncated and slightly elongated summit marked by a 400-m-diameter, 300-m-deep crater.

Citlaltépetl is the highest peak of Mexico and third highest of North America, with an elevation of 5675 m asl. It rises 2900 m above the Highlands to the west and 4300 m above the Coastal plain of the Gulf of Mexico to the east. Citlaltépetl has a complex eruptive history that was first described by Robin and Cantagrel (1982) and later outlined by Carrasco-Núñez (1992) and Höskuldsson (1992). Carrasco-Núñez (1993) proposed a four-stage model that involves the construction of three superimposed cones and the emplacement of several outer silicic domes.

The historical eruptive record of Citlaltépetl Volcano reveals intense effusive and explosive activity during the 16th and 17th centuries (Mooser et al., 1958; Waitz, 1910) and mainly fumarolic activity for the last 300 years (Crausaz, 1986; Crausaz, 1994). Although there is an abundance of effusive rocks in the recent record

* Corresponding author

SSDI 0377-0273(95)00023-2

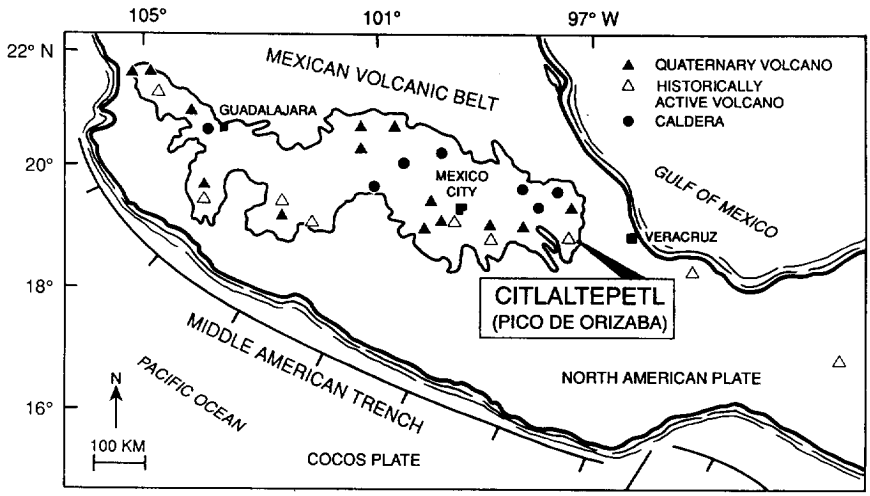

Fig. 1. Location of Citlaltépetl volcano at the eastern end of the Mexican Volcanic Belt.

at Citlaltépetl, numerous pyroclastic deposits were also erupted during the Late Pleistocene and Holocene. This paper focuses on the young pyroclastic rocks, particularly on Holocene scoria-and pumice-flow deposits, as part of an effort to understand the types, extent, and frequency of volcanic hazards that Citlaltépetl presents. Previous studies of the Holocene pyroclastic-flow units (Robin et al., 1983; Cantagrel et al., 1984; Höskuldsson and Robin, 1993) suggested that there were several repetitive periods of activity separated by intervals lasting 1000–1500 years. One of the conclusions of this new study is that most of the Holocene pyroclastic-flow units of Citlaltépetl are part of a single eruptive episode that took place between 8500 and 9000 yr. B.P. The deposits underlie several important cities, including Orizaba; therefore knowledge of these deposits, their origin, and emplacement mechanisms is important for hazard assessment.

2. General character of the deposits

Most of the young pyroclastic sequences identified at different areas around Citlaltépetl Volcano are similar in composition, structure, relative stratigraphic position, and apparent absence of unconformities among successive eruptive units. Based on extensive examination of these features, in the field and laboratory, we have correlated these on all flanks of Citlaltépetl. Radiocarbon dating of charcoal within these deposits confirmed the working hypothesis that most of the studied pyroclastic-flow units could be associated with a single eruptive episode that lasted a few hundred years.

The deposits are irregularly distributed around the Citlaltépetl summit crater, forming discrete tongues that are mainly confined to river-valleys, except on the western flank where they form an open-valley deposit with a fan-like shape (Fig. 2). At least six transport trails can be traced, delineating the distinct paths followed by the pyroclastic flows (Fig. 2). The erupted material was channeled on the lower slopes of the northeast, east, southeast, and south flanks of the volcano, where the slope is greater than on the western flank, leaving discontinuous deposits with variable thicknesses, which, in most cases, increase downstream in valleys or local topographic depressions.

An estimate of the total erupted volume represented by these deposits was made by summing the volumes at individual outcrops. The estimated volume is about 0.37 km^3 of bulk erupted material, equivalent to 0.26 km^3 dense rock equivalent using an averaged density factor of 0.7.

The deposits are composed of a set of successive pyroclastic-flow units that were emplaced during a short time interval and are compositionally homogeneous, forming a single eruptive unit as defined by Freundt and Schmincke (1985). They are typically unconsolidated, low-grade ignimbrites (Walker, 1983), which do not show a defined flow front or lateral

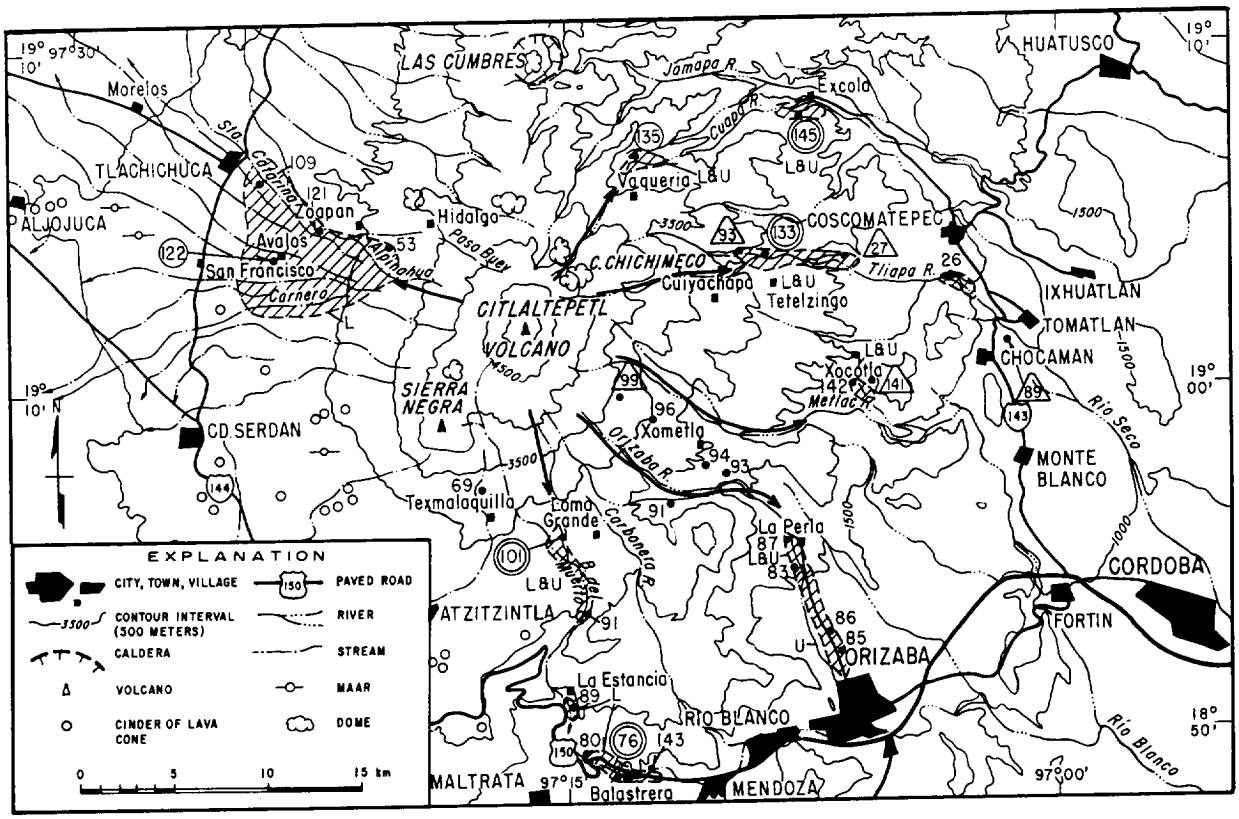

Fig. 2. Distribution map of the Citlaltépetl ignimbrite deposits (diagonals). Arrows indicate suggested flow paths. Numbers indicate sampling sites: circled numbers locate key sections shown in Fig. 4, double circle where ^{14}C date is available, and triangles for other deposits with ^{14}C (Table 3). Labels indicate stratigraphic members: L = Lower; U = Upper member; and $L\&U$ = both members.

levees and have smoothly undulating, relatively flat upper surfaces that are sometimes slightly inclined, reflecting the underlying topography. We initially named the deposit 'Citlaltépetl scoria-and- pumice-ash flow', following the genetic classification of pyroclastic flows proposed by Wright et al. (1980), since they are composed of variable proportions of both andesitic scoriae and pumices of various compositions, but with a slightly higher abundance of the former. However, we decided to adopt the term 'Citlaltépetl ignimbrite' for simplicity, even though the deposit does not just contain pumice fragments.

The Citlaltépetl ignimbrite is subdivided into lower and upper members. The contacts between members are conformable and do not show any indication of erosion. Although both members are generally similar in composition, they differ in the number of individual flow units, their internal structure, and their distribution. A summary of the characteristics of each member is given in Table 1. The transition between members is marked by a distinctive pumice-fall layer. Each member has particular features that vary not only within the stratigraphic sequence, but also with distance from vent.

3. Field descriptions of the deposits

3.1. Lower member

The Lower member reaches distances of up to 30 km from the crater in all directions. It shows a complex stratigraphy that is more evident at localities closer to the volcano such as: Vaquería, 10.7 km northeast (sampling site 135, Fig. 3), Loma Grande, 12 km south (sampling site 101, Fig. 3), and Excola, 18 km northeast (sampling site 145, Fig. 3), where several flow units are present. On the western flank (Avalos locality,

Table 1
General features of the Citlaltépetl ignimbrite's members

Unit		Lower member	Upper member
Definition		multiple flow units	single flow unit
General Stratigraphy	top	scoria-pumice flow unit laharic unit	scoria-pumice flow unit pumice-fall unit
	bottom	two scoria-pumice flow units	
Structures:	degassing pipes	abundant on flow tops	scarce
	pumice lenses	common at proximal zones	on flow bottom at distal zones
	lithic lenses	common at proximal zones	none
	red-colored tops	at distal zones	not well-defined
Distribution	proximal zone (< ~ 13 km)	all directions	all directions but W
	distal zone (> ~ 13 km)	all directions	NE, E, and SE directions

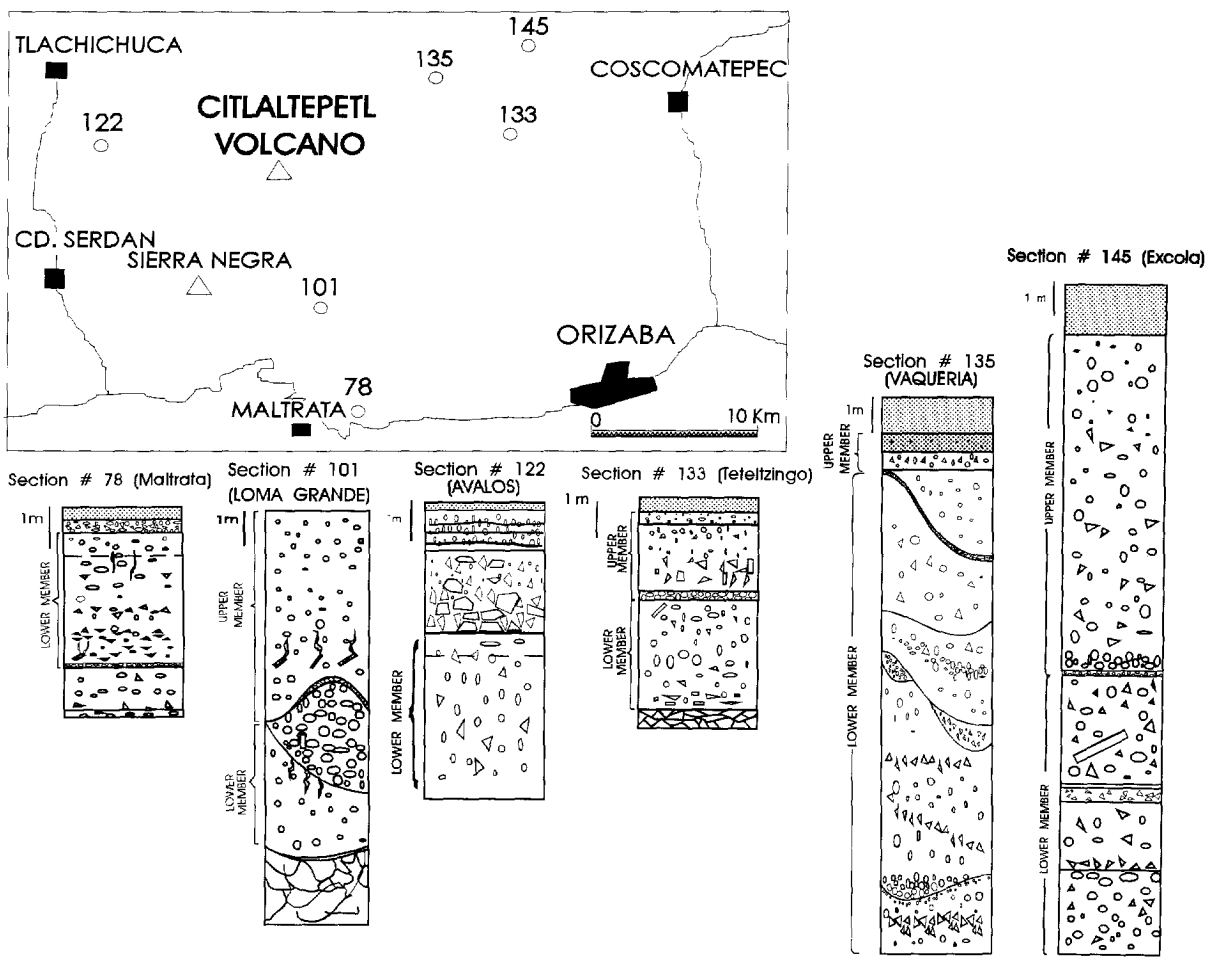

Fig. 3. Location of outcrops and stratigraphic relationships of different sections measured across the Citlaltépetl ignimbrite deposit (see Fig. 4 for descriptions of sections and symbols).

Fig. 3) and at greater distances on the south flank (Maltrata locality, Fig. 3) the deposit consists of a single flow unit.

At Excola, the Lower member shows its most complex stratigraphy (Fig. 4a). It is a multiple flow unit with two pyroclastic flow deposits at the base, a laharic deposit with an incipient thin soil barely visible on its top, and an overlying pumice-flow deposit. The basal pyroclastic-flow deposit is 2.5 m thick and contains in order of abundance: scoriae, pumices, and lithics. Scoria clasts are dense, black, subrounded, and mostly block-sized (the largest clasts: 70 cm in diameter). Pumices are usually rounded and consist of several types. Most common are blocky and lapilli-sized, highly vesiculated pumices (largest clasts: 40 cm in diameter). Banded pumices, usually rounded and blocky-lapilli-sized (largest clasts: 30 cm in diameter), contain fine layers composed of different proportions of black scoria, black pumice, white pumice, and mixed layers of grey and brown pumice. A crude reverse grading of scoria and pumice fragments is observed; the upper half is typically coarser than the lower half, which contains more lapilli-sized clasts with the largest block only about 20 cm in diameter. Overlying this deposit, with a quasi-planar contact, is a second scoria-and-pumice-flow deposit. It has a thickness of 1.8–2.0 m and contains pumices similar to those in the lower deposit. In contrast, it is slightly welded and contains clasts of much smaller size (largest clast is only 20 cm) and has a smaller proportion of both pumice and scoria fragments, and more abundant gravel-sized lithic clasts. Scoriae in this deposit are more abundant than banded pumices. Lithics are concentrated at the bottom of the flow unit, forming a 6-cm-thick, laterally discontinuous layer made only of lithic clasts. Overlying the younger pyroclastic-flow deposit is a 0.75-m-thick succession of several stratified laharic and fluviatile units. On top of this reworked deposit there is a 10-cm-thick, poorly developed soil, which may represent a brief break in the emplacement of successive pyroclastic flows. This soil layer is capped by a 3.3-m-thick scoria-and-pumice- flow deposit, which contains abundant large charcoalized logs, some of them with associated degassing pipes. The latter deposit has the same relative proportions of scoriae and pumices (60–40%) as the basal deposit.

In the distal zone on the southern flank of Citlaltépetl Volcano (see Maltrata section, Fig. 4b), the lower member is composed of a single flow unit, consisting of a basal ground surge layer, the main flow unit, and a thin (10-cm-thick) ash-cloud layer on top, a sequence corresponding to layers 1, 2 and 3 of the standard pyroclastic-flow scheme proposed by Sparks et al. (1973). The simpler stratigraphy suggests that not all of the flows that are found at Excola reached Maltrata (Fig. 4b) and Avalos (Fig. 4c). A basal layer is only observed at Maltrata, where it is typically in sharp and undulating contact with the overriding main flow unit of the Lower member. This layer can be divided in two subunits, the lower one is a 5–10-cm-thick fall-like deposit that contains mainly well-sorted, yellow pumices. The upper one is only 3–4 cm thick and faintly laminated: in some places it has cross-bedded, surge-like structures with yellow pumices and abundant sand to silt-sized lithics.

The main flow unit at Maltrata and Avalos has a characteristic, altered, yellow-colored horizon at the top that contrasts with a reddish-brown and thicker horizon in the lower part. The deposit usually shows a crude reverse grading of scoriae and both dark and light-colored pumices. Lithics are mainly concentrated in the lower half of the deposit, forming a 0.45–3-m-thick, highly concentrated horizon of pebble-granule-sized particles near the bottom. Lithics in the upper part of the deposit are generally monolithologic, consisting mostly of angular, pale-grey hornblende-bearing glassy dacite clasts; in contrast, the lower part is more heterolithologic. The upper part of the reddish brown horizon contains, in most of the cases, numerous gas segregation structures (Maltrata section, Fig. 4b), which in some places (Loma Grande, Fig. 4d) are truncated by subsequent flow units, suggesting a continuous emplacement of pyroclastic flows.

Additional features are observed at other localities. At Loma Grande (Fig. 4d), 12 km upstream of Maltrata, there are two flow units. The upper unit has a pumice-rich zone at the flow front. At Vaquería (Fig. 4e), 7.2 km upstream of Excola (Fig. 3), the deposit consists of several flow units. These appear to correlate with those described at Excola, although they contain a higher proportion of lithics, particularly the lower units, which are mostly clast-supported. In addition, flow units at Vaquería include multiple lithic-rich or pumice-rich concentration lenses at different levels of the sequence. Lee-side pumice lenses are found 2

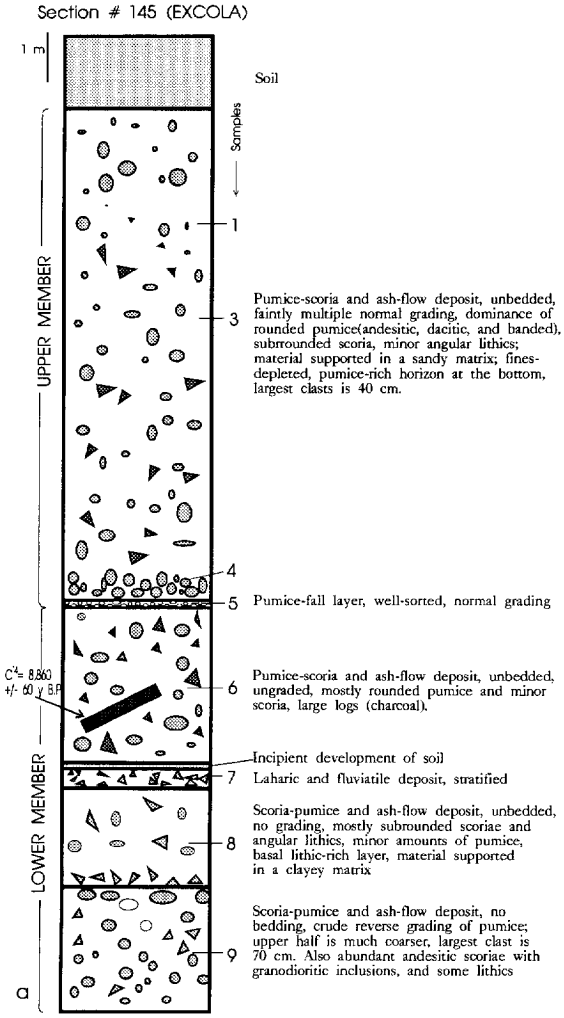
Section # 145 (EXCOLA)
1 m
Soil
Samples
UPPER MEMBER
LOWER MEMBER
1
3
Pumice-scoria and ash-flow deposit, unbedded, faintly multiple normal grading, dominance of rounded pumice(andesitic, dacitic, and banded), subrounded scoria, minor angular lithics; material supported in a sandy matrix; fines-depleted, pumice-rich horizon at the bottom, largest clasts is 40 cm.
4
5
Pumice-fall layer, well-sorted, normal grading
C14= 8,860 +/- 60 y B.P.
6
Pumice-scoria and ash-flow deposit, unbedded, ungraded, mostly rounded pumice and minor scoria, large logs (charcoal).
Incipient development of soil
7
Laharic and fluviatile deposit, stratified
8
Scoria-pumice and ash-flow deposit, unbedded, no grading, mostly subrounded scoriae and angular lithics, minor amounts of pumice, basal lithic-rich layer, material supported in a clayey matrix
9
Scoria-pumice and ash-flow deposit, no bedding, crude reverse grading of pumice; upper half is much coarser, largest clast is 70 cm. Also abundant andesitic scoriae with granodioritic inclusions, and some lithics
a

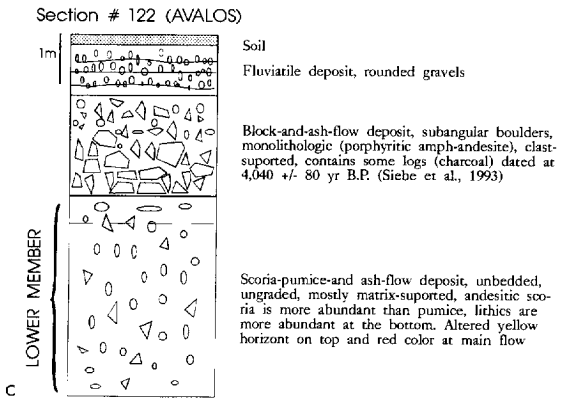
Section # 122 (AVALOS)
1m
Soil
Fluviatile deposit, rounded gravels
Block-and-ash-flow deposit, subangular boulders, monolithologic (porphyritic amph-andesite), clast-suported, contains some logs (charcoal) dated at 4,040 +/- 80 yr B.P. (Siebe et al., 1993)
LOWER MEMBER
Scoria-pumice-and ash-flow deposit, unbedded, ungraded, mostly matrix-suported, andesitic scoria is more abundant than pumice, lithics are more abundant at the bottom. Altered yellow horizont on top and red color at main flow
c

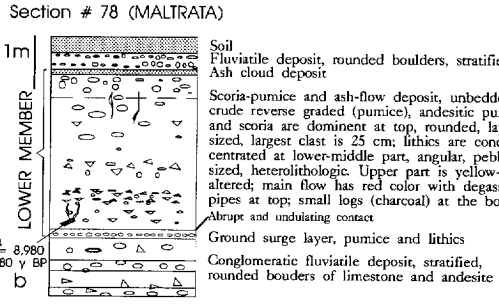
Section # 78 (MALTRATA)
1m
Soil
Fluviatile deposit, rounded boulders, stratified
Ash cloud deposit
LOWER MEMBER
Scoria-pumice and ash-flow deposit, unbedded, crude reverse graded (pumice), andesitic pumice and scoria are dominent at top, rounded, lapilli-sized, largest clast is 25 cm; lithics are concen-centrated at lower-middle part, angular, pebble-sized, heterolithologic. Upper part is yellow-altered; main flow has red color with degassing pipes at top; small logs (charcoal) at the bottom
Abrupt and undulating contact
Ground surge layer, pumice and lithics
C14= 8,980 +/-80 y BP
Conglomeratic fluviatile deposit, stratified, rounded bouders of limestone and andesite
b

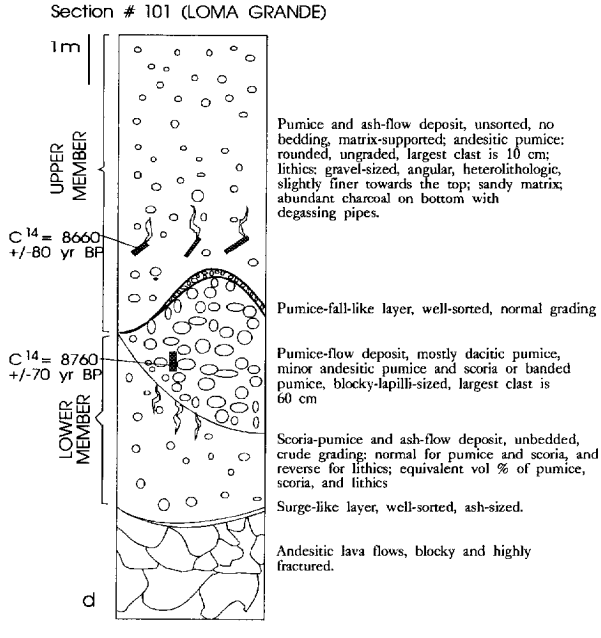
Section # 101 (LOMA GRANDE)
1m
UPPER MEMBER
Pumice and ash-flow deposit, unsorted, no bedding, matrix-supported; andesitic pumice: rounded, ungraded, largest clast is 10 cm; lithics: gravel-sized, angular, heterolithologic, slightly finer towards the top; sandy matrix; abundant charcoal on bottom with degassing pipes.
C14 = 8660 +/-80 yr BP
Pumice-fall-like layer, well-sorted, normal grading
C14 = 8760 +/-70 yr BP
Pumice-flow deposit, mostly dacitic pumice, minor andesitic pumice and scoria or banded pumice, blocky-lapilli-sized, largest clast is 60 cm
LOWER MEMBER
Scoria-pumice and ash-flow deposit, unbedded, crude grading: normal for pumice and scoria, and reverse for lithics; equivalent vol % of pumice, scoria, and lithics
Surge-like layer, well-sorted, ash-sized.
Andesitic lava flows, blocky and highly fractured.
d

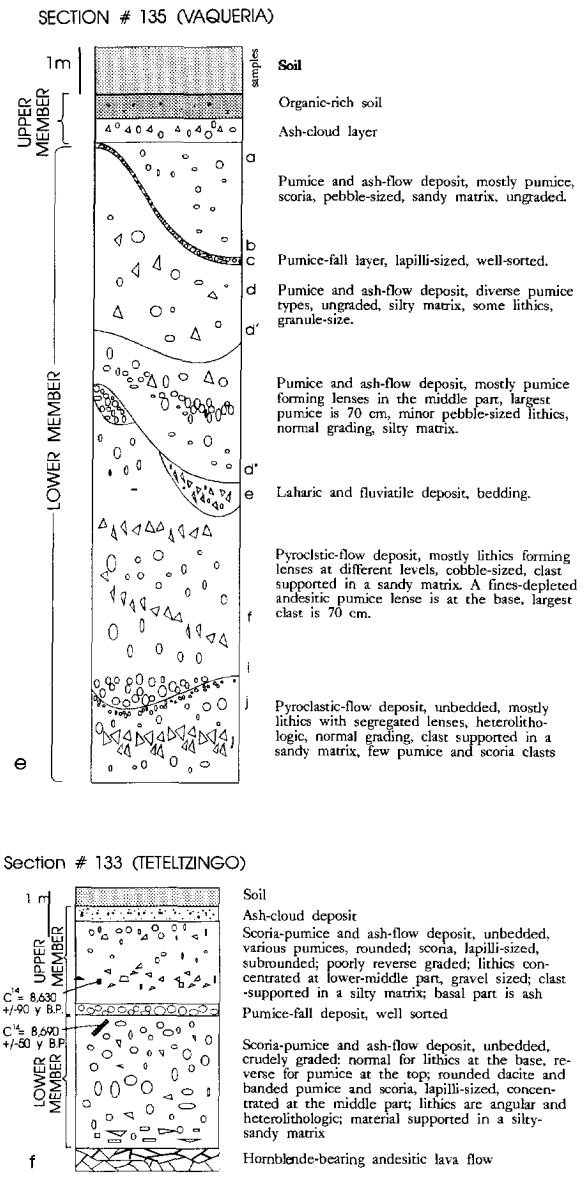

Fig. 4. Selected stratigraphic columns of outcrops discussed in the text (for location see Fig. 3).

km upstream of Maltrata, associated with low topographic obstacles.

3.2. *Upper member*

The upper member consists of a basal pumice-fall layer, and a single pyroclastic-flow deposit that sometimes includes an overriding ash-cloud horizon. The pumice-fall layer consists of well-sorted, lapilli-sized, mostly yellow pumices and a minor proportion of lithics, which commonly show prismatic jointing. In some places, this layer has reversely graded pumices (Excola locality, Fig. 4a). Its thickness typically ranges from 14 cm (22 km southeast from the vent) to 25 cm (18 km southeast).

The overlying flow unit is typically ungraded, unbedded, and mostly matrix-supported, although in some places it is gravel-supported with a sand-silt matrix. It consists mostly of black scoriae, black and brown pumices, and relatively minor proportions of banded pumices (black and white or brown and white colors), pale-brown and white-yellow pumices, and a variety of lithics. Most of the particles are lapilli-sized, but there are frequent occurrences of blocks, which in some cases are preferentially distributed either at the bottom or at the top, showing faint reverse or normal grading. The largest pumice clast observed was about 40 cm in diameter. The thickness of the flow unit varies from approximately 2 m (Teteltzingo, Fig. 4f) to 10 m (Excola, Fig. 4a).

Most dark-colored pumices and scoriae are rounded or subrounded clasts, generally with low vesicularity. They contain some crystals of hornblende in a glassy matrix, as well as numerous angular, dense, juvenile dacite inclusions of characteristic white or pale-grey color that contrasts with the black or brown pumices. However, scoria clasts are always denser than pumice clasts. Dark-colored pumices are usually black and sometimes brown. Light-colored pumices contain hornblende phenocrysts and are always very vesicular; however when associated with dark pumice in banded samples, the vesicularity is substantially less. The light-colored pumice clasts are common in the upper part of the deposit, but they can also be concentrated at the bottom forming a basal fines-depleted layer (Excola site, Fig. 4a), which resembles the ground layer found at the base of the Taupo ignimbrite (Wilson and Walker, 1982). Lithics are mostly angular, heterolithologic and preferentially concentrated toward the lower part of the flow unit. Charcoal and sometimes large logs are present close to the bottom of the flow unit and these sometimes are associated with gas segregation pipes.

4. Grain-size characteristics

Samples from different sites and distinct stratigraphic units were sieved in order to observe vertical

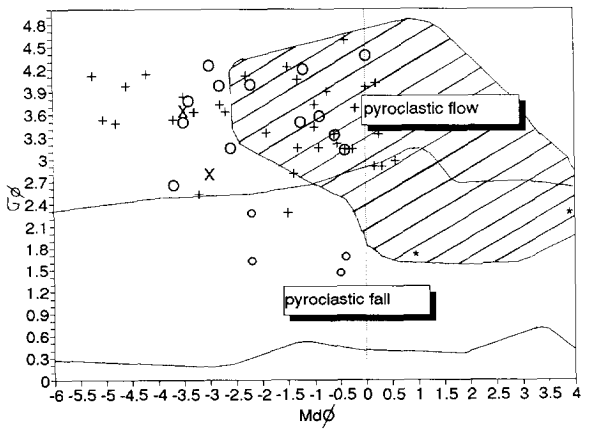

Fig. 5. Md_ϕ/σ_ϕ plot (after Walker, 1971) of the Citlaltépetl ignimbrite deposits. Symbols for Upper member: large circles = scoria-pumice flow deposits; small circles = pumice-fall layer; Lower member: plus signs = scoria-pumice flow deposits; crosses = lahar; asterisks = surge layer.

grain-size variations. For some samples we did component analysis of each size class down to 0.5 mm by hand-picking and weighing of splits, and by grain-counting with a binocular microscope for the finer classes. Because scoriae, dark-color pumices, and lithics in fractions finer than 0.5 mm show a similar appearance, component analysis is not reliable for these classes. Inman parameters such as median diameter ($Md_\phi = \phi_{50}$) and sorting index ($\sigma = \phi_{84} - \phi_{16/2}$) were obtained from histograms and cumulative frequency curves.

Because most samples represent flow-type units, they are typically poorly sorted with σ_ϕ values ranging from 2.6 to 4.6, but mainly between 3.0 and 4.0. Therefore, nearly all the flow-type samples lie within the pyroclastic-flow field on the Md_ϕ-σ_ϕ diagram (Walker, 1971) (Fig. 5). Some flow samples plot outside this field because they are much coarser. In contrast, pumice-fall samples from the base of the Upper member are comparatively well-sorted and plot within the pyroclastic-fall field, and the surge layers forming the base of the Lower member have a low sorting index and are comparatively finer than the other samples.

The grain-size distributions of samples from the Citlaltépetl ignimbrite at Excola (Fig. 6) show a distinctive Gaussian distribution for the pumice-fall layer, at least 2 main subpopulations for the scoria-and-pumice-flow samples of the Upper member, and no less than 3 subpopulations for the Lower member (Fig. 6). Sheridan et al. (1987) proposed that the observed subpopulations in pyroclastic-flow deposits may represent the overlap of different transportation modes of particles. Crystals are present for grain size classes <0.5 mm in most of the samples. The proportion of pumices and scoriae is higher than lithics throughout the Upper Member. The basal part of the Upper member is a fines-depleted, pumice-rich horizon (see histogram #4 in Fig. 6), whereas lithics are particularly concentrated at the lower and middle parts of the layer 2 in the Upper member.

The proportions of components differ for each flow unit in the Lower member (Fig. 6). In the uppermost scoria-flow unit pumice is more abundant (4:1) than scoria. The laharic and fluviatile units have a dominance of lithics over all other components. The lower middle flow unit exhibits a similar proportion of scoria-pumice and lithics (4:3), even though lithics are relatively dominant at the bottom. The lowermost unit contains a lot of blocky-sized scoria and pumice fragments in a proportion of about 3 to 2, whereas lithics are more abundant in smaller size classes.

5. Petrography

Scoria samples commonly contain, in order of abundance, phenocrysts (1–2 mm in maximum diameter) plagioclase, microgranodiorite xenoliths, microphenocrysts (0.2–0.5 mm in maximum diameter) of clinopyroxene, orthopyroxene and amphibole, and accidental lithics. Petrographic observations of different scoria and pumice samples reveal clear evidence of mineralogical and textural disequilibrium. There are some sporadic occurrences of olivine and quartz, which are particularly present in grey or light-brown pumice fragments. Olivine always has reaction rims of clinopyroxene and amphibole, and quartz has a reaction corona, unequivocal evidence that it is a xenocryst. The matrix is composed mostly of dark-brown glass that sometimes exhibits a flowage texture.

Based on the shape, habit, and zoning, at least two different types of plagioclase can be identified. Type 1 consists of smaller and sometimes partially broken crystals of mainly labradorite and andesine with euhedral to subhedral shapes and tabular habits, sometimes showing either oscillatory or normal zoning. In contrast, type 2, which is more abundant, is mostly com-

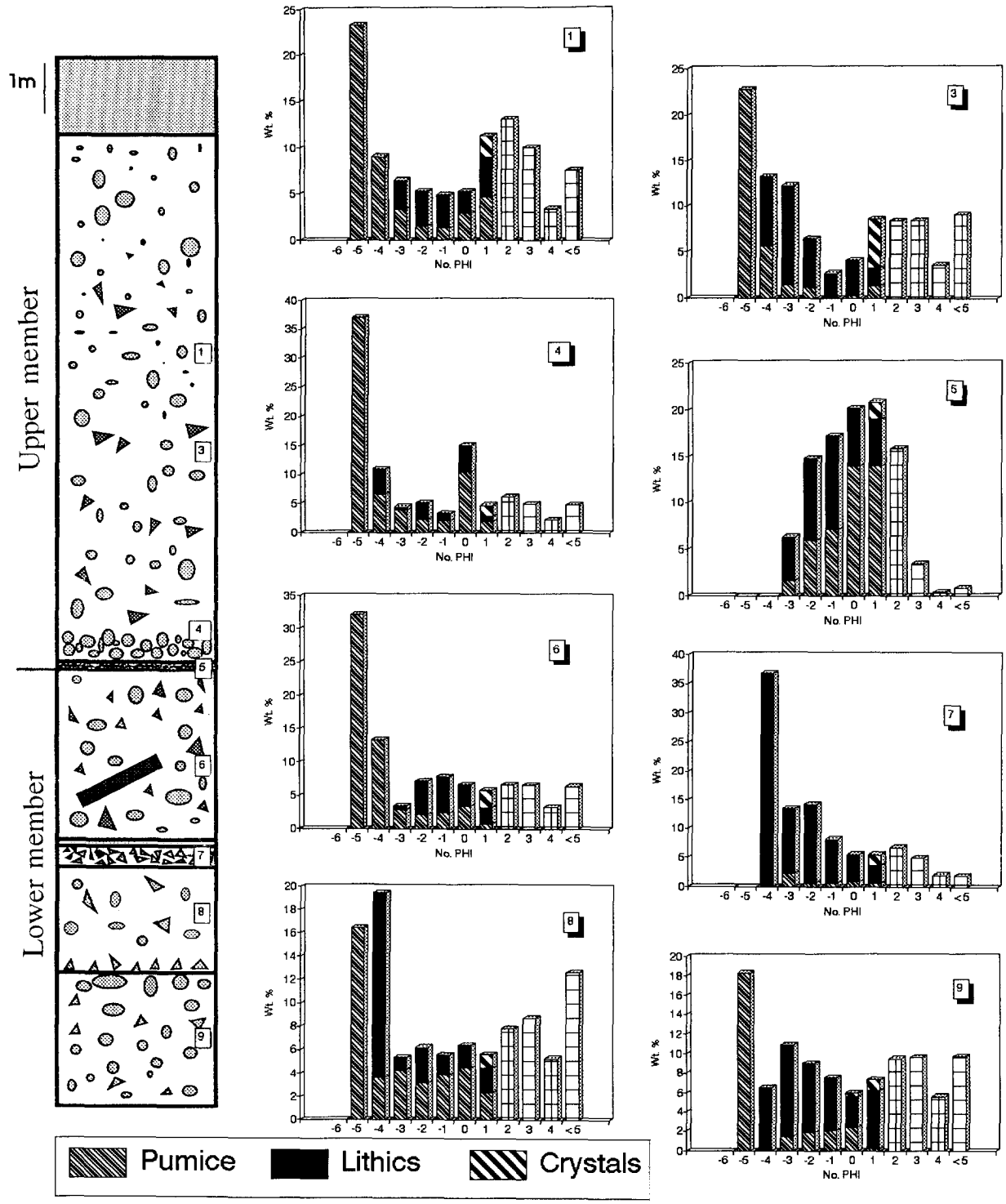

Fig. 6. Grain-size histograms of pyroclastic samples at Excola locality. Stratigraphic column illustrates the position of each sample. Description of deposits can be found in Fig. 4a. All samples are of flow-type except #5 (fall-type) and #7 (lahar). Component analysis was performed for fractions of 0.5 mm and coarser. Grid pattern represents undifferentiated components. Pumice pattern include both pumice and scoria particles.

posed of oligoclase-andesine, and exhibits truncated shapes with reverse or complex oscillatory zoning. They contain abundant glass inclusions, especially at crystal cores, forming either skeletal, sieve-like, or dusty/cellular habits. These textures have been interpreted in other localities as due to resorption processes occurring during magma mixing (Dungan and Rhodes, 1978; Eichelberger, 1978; Tsuchiyama, 1985; Halsor, 1989).

Pyroxenes are small and frequently found in clusters, sometimes associated with euhedral titanomagnetite, glass-inclusion-bearing plagioclases (Type 2), and amphiboles. Amphibole crystals in scoria samples generally have well-defined contacts, but in dacitic pumices they usually have oxide-reaction rims.

The microgranodioritic inclusions have sharp and nearly planar contacts with the glassy matrix of the scoriaceous material, and do not exhibit any evidence of reaction, suggesting a rapid ascent to the surface. They are holocrystaline and contain mostly euhedral, quasi-tabular, inclusion-free plagioclase crystals in the form of phenocrysts, microphenocrysts or cryptocrystals forming a seriate or sometimes porphyritic texture. Plagioclase (oligoclase-andesine) sometimes shows truncated oscillatory zoning and intergrowths with other plagioclase crystals. Biotite and amphibole are occasional accessory minerals, usually isolated and smaller. Pyroxene crystals are also present, commonly associated with opaques, and in some cases showing rounded and reacted rims suggesting xenocrystic origins. Because local basement, composed of limestone and shale, was apparently not sampled by the ascending magma, we believe that the granodioritic inclusions represent the walls of a shallower magmatic reservoir.

6. Chemical composition

Major-element analyses of pumice and scoria samples (Table 2) were performed using X-ray fluorescence techniques at the Washington State University Geoanalytical Laboratory. The precision and accuracy of the chemical analyses are comparable or better than other XRF laboratories (Hooper, 1964; Hooper and Atkins, 1969). The observed low total values in most samples reflect undetermined LOI. Four types of pumice and scoriae were distinguished: (1) light-colored pumices, mainly white; (2) brown pumices, and

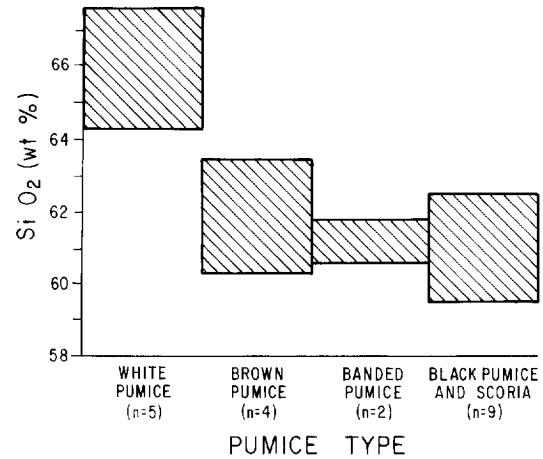

Fig. 7. Silica content ranges for juvenile components in the Citlaltépetl ignimbrite deposit.

banded pumices, including finely laminated pumices of light, dark, and sometimes intermediate color; (3) dark, mostly black pumices and nonvesiculated scoriae; and (4) felsic inclusions inside both scoriae and black pumices (Fig. 7). Classification based on total alkalies versus silica (Le Bas et al., 1986) shows that all samples are subalkalic and all the black pumices and scoriae are andesitic, whereas white pumices are mainly dacites with only a single sample in the rhyolite field (Fig. 8). Brown pumices and banded pumices include both

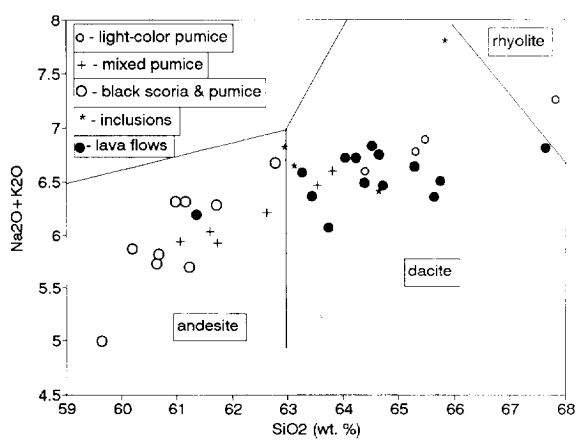

Fig. 8. Diagram of wt% alkalies ($Na_2O + K_2O$) versus wt.% SiO_2 for the Citlaltépetl ignimbrite deposit and recent lava flows (younger than 5000 yr. B.P.). Rock names based on nomenclature used by Le Bas et al. (1986). Data for lava-flow samples are from Carrasco-Núñez (1993).

Table 2
Chemical analyses of pumice, scoria, and inclusion clasts. The samples can be located by numbered site in Fig. 2.

Type:	incl.	incl.	w.p.	incl.	b.p.	b.p.	b.p.	b.p.	b.s.	b.s.	b.s.	b.s.
Sample:	99	135e	135b	135j	135d	145f	145g	135a	135c′	78	145e	145h
SiO_2	62.03	62.69	63.95	65.36	59.67	59.63	60.41	60.91	58.47	59.40	60.35	61.09
TiO_2	0.65	0.73	0.65	0.50	0.82	0.77	0.78	0.80	0.82	0.76	0.76	0.77
Al_2O_3	16.32	18.31	16.47	16.10	15.74	16.32	16.32	16.08	17.15	16.01	16.40	16.79
FeO^T	4.69	4.52	3.75	3.72	5.58	5.81	5.79	5.57	5.24	5.68	5.31	5.27
MnO	0.09	0.08	0.08	0.07	0.10	0.10	0.10	0.10	0.10	0.10	0.09	0.09
MgO	2.61	1.69	2.06	2.03	3.63	3.86	3.81	3.61	3.79	3.68	3.62	2.87
CaO	5.22	4.50	5.39	4.54	5.91	6.61	6.57	6.01	6.43	6.43	6.25	5.72
Na_2O	4.51	4.93	4.47	5.53	3.92	4.06	3.96	4.10	3.35	3.90	3.77	4.27
K_2O	2.00	1.85	1.85	2.19	2.26	1.75	1.75	2.19	1.55	1.80	1.85	1.95
P_2O_5	0.19	0.23	0.27	0.16	0.25	0.19	0.19	0.20	0.17	0.19	0.19	0.20
Total	98.30	99.61	98.94	99.28	97.88	99.10	99.68	99.57	97.07	97.95	98.59	99.02

Type	b.s.	br.p.	br.p.	br.p.	br.p.	ba.p.	ba.p.	w.p.	w.p.	w.p.	w.p.
Sample	133b	135d′	135d″	135f	145a	145c	145b	135i	145i	135c	145d
SiO_2	61.69	60.35	62.67	62.99	61.96	60.71	61.09	64.06	64.31	64.41	66.82
TiO_2	0.70	0.83	0.57	0.58	0.65	0.70	0.71	0.58	0.53	0.50	0.37
Al_2O_3	16.34	16.23	17.71	17.21	16.96	16.15	16.13	16.72	16.56	16.74	16.29
FeO^T	4.83	5.71	4.24	4.20	4.83	5.34	5.40	4.27	3.87	3.71	2.97
MnO	0.09	0.10	0.08	0.08	0.09	0.09	0.09	0.08	0.08	0.07	0.07
MgO	2.64	3.65	1.94	2.02	2.91	3.44	3.54	2.09	1.72	1.54	1.15
CaO	5.21	5.85	4.84	4.92	5.61	6.01	6.05	4.90	4.54	4.43	3.63
Na_2O	4.41	3.75	4.57	4.60	4.25	4.06	3.99	4.54	4.63	4.73	4.88
K_2O	2.15	2.13	1.82	1.93	1.91	1.90	1.85	2.04	2.06	2.06	2.28
P_2O_3	0.24	0.26	0.21	0.21	0.20	0.19	0.19	0.21	0.20	0.20	0.17
Total	98.30	98.86	98.65	98.74	99.37	98.59	99.04	99.49	98.50	98.39	98.63

Key: incl. = inclusions, b.p. = black pumice, b.s. = black scoria, br.p. = brown pumice,ba.p. = banded pumice, w.p. = white pumice.

andesite and dacite (plotted as 'mixed' pumice in Fig. 8) and these plot between the black and white pumices. Inclusions found within scoriae and andesitic pumices are chemically classified as microgranodiorite (quartzdiorite) and plot in or very near the dacite field. For comparison, recent lavas of Citlaltépetl are almost all dacites.

Banded and brown pumices, which are compositionally intermediate between apparent end-members andesite and dacite, are closer to the andesitic member suggesting that this magma was apparently more voluminous in mixes than the silicic magma. This interpretation agrees with the relative higher volume of black scoriae and pumice over white pumices in the deposit as a whole. A nearly linear trend is observed for pumice and scoria samples when SiO_2 is plotted versus MgO (Fig. 9). Similar trends are also observed for TiO_2, FeO^*, MgO, CaO, Na_2O, and K_2O. Mixed pumice, including both brown and banded types, plot approximately in the middle of these trends (Fig. 9).

Scoriae and pumices were sampled from different stratigraphic levels within the deposits to test whether their compositions changed with time of emplacement. Although a variety of pumices and scoriae are present in the deposits, stratigraphic trends do seem to occur for samples that, because of their relative higher abundance, we consider representative of each deposit (Fig. 10). At the base of the Lower member dacitic pumices are dominant while more mafic compositions upward, where andesitic pumices are more abundant in the uppermost part. In the pumice-fall at the base of the Upper Member, simultaneous deposition of both dacitic and andesitic pumices took place in approximately similar proportion. The Upper member also followed a progressively more mafic trend above the pumice fall. Only three microgranodiorite inclusions found within

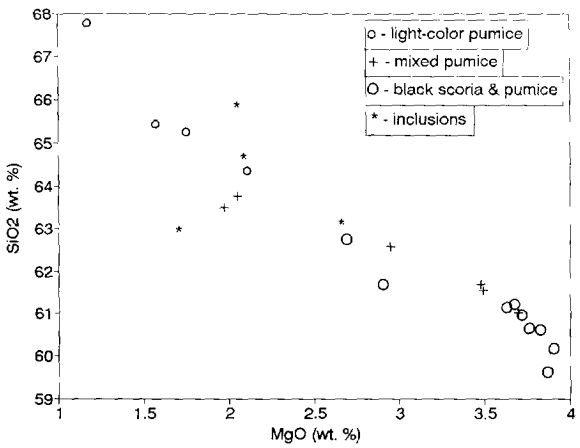

Fig. 9. Plot of wt.% SiO_2 versus MgO for pyroclastic material from Citlaltépetl volcano.

scoria clasts were sampled at different stratigraphic levels (Table 2). Stratigraphic trends for the compositions of these inclusions are less well defined, but SiO_2 and K_2O show a progressive decrease towards the top of the sequence, whereas FeO total, CaO, MgO, TiO_2, and MnO values tend to increase. The inclusions, only found in the scoriaceous material, may represent the upper parts of a magmatic reservoir that was probably emplaced at shallow levels prior to the Citlaltépetl ignimbrite's eruption. No other rocks were sampled by the eruption with the exception of the surface or near-surface rocks, which were incorporated during the eruptive event.

The chemical variations observed for the pumices, scoriae, and microgranodiorite inclusions suggest the existence of a compositionally zoned dacitic reservoir. This reservoir apparently had periodic resupply of andesitic magma, which may have triggered explosive eruptions, as proposed by Sparks et al. (1977).

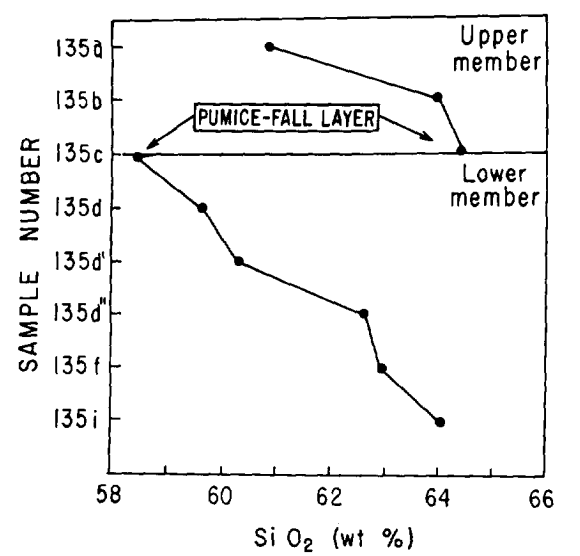

Fig. 10. Silica content variation with time (stratigraphic position) of representative pumice and scoria samples at Vaquería locality (Fig. 4e). Progressive decreases in silica are observed for samples of both the Lower and Upper members. Samples of the pumice-fall layer (Upper member) include both high- and low-silica types, bridging these trends.

7. Radiocarbon dates

Field observations were fundamental in determining the stratigraphic relationships among the recent pyroclastic sequences observed around Citlaltépetl volcano. Due to the apparent similarities in composition and depositional structures in pyroclastic-flow deposits located in different areas, we suspected that a correlation among them was viable. Furthermore, because no erosional contacts are found among successive pyroclastic-flow units, we believed they should be formed over a short period of time.

To confirm this hypothesis and in order to correlate deposits of different areas around the volcano, we sampled organic material such as charred logs and branches included in the pyroclastic-flow deposits for radiocarbon dating. Analyses were performed by the Beta Analytic Laboratories (Coral Gables, Florida, U.S.A.). Table 3 lists ^{14}C dates for the Citlaltépetl ignimbrite deposit at different localities as well as other recent deposits of Citlaltépetl volcano. For the Citlaltépetl ignimbrite, we did not include the date of 8300 ± 70 yr.B.P. reported by Höskuldsson and Robin (1993) because the same deposit was also dated at 8470 ± 160 yr. B.P. by Siebe et al. (1993) (Table 3). Therefore, the dates for the Citlaltépetl ignimbrite range from about 8455 to 8980 yr. B.P. and demonstrate similar but not precisely uniform ages (Fig. 11). They yield an average age and relative standard deviation of 8795 ± 57 yr. B.P. for the Lower member, and of 8573 ± 79 yr. B.P. for the Upper member. The relative standard deviation represents the error for multiple measurements and was calculated using two sigma to produce a 95% confidence. Errors for each date were

Table 3
Radiocarbon dates of the Citlaltépetl ignimbrite deposits and other recent deposits

Member	Sample	C^{14} dates	Deposit	Location	Long.	Lat.	Reference
–	A83.1	690 ± 50	p.fall	El Jacal	?	?	1
–	HV14365	1730 ± 85	r.af	Zoapan	97 22.8′	19 04.7′	2
–	A75.2	1810 ± 50	a.fall	San Jose	?	?	1
–	A78.2	1860 ± 40	b&af	Texmalaquilla	?	?	1
–	A78.3	1910 ± 40	s&af	Texmalaquilla	?	?	1
–	PU-132	3400 ± -110	lava	Orizaba	?	?	3
–	A84-1	3450 ± 70	p.fall	El Jacal	?	?	1
–	9015	4040 ± 80	r.b&af	Avalos	97 24.5′	19 03.5′	4
–	PU-139	4060 ± 120	p.fall	Summit	?	?	3
–	9017	4090 ± 90	b&af	B. Carnero	97 23.2′	19 02.8′	4
–	PO-47′	4200 ± 80	b&af	Avalos	97 19′	19 02′	This study
–	HV14321	4450 ± 70	pf	Zoapan	97 22.8′	19 05′	2
–	9004	4660 ± 100	b&af	Avalos	97 23′	19 04′	4
Upper*	PU-127	6200 ± 120[a]	s&af	Loma Grande	97 14.9′	18 55.2′	3
–	A80.1	6640 ± 290[a]	b&af	Metlac	?	?	1
Upper*	PU110b	7020 ± 120[a]	s&af	Tliapa	97 07.3′	19 09.6′	3
–	PA72.2	8170 ± 70[b]	b&af	Loma Grande	?	?	1
Upper ?	A74	8300 ± 70[b]	s&af	B. Carnero	?	?	1
Upper	HV14320	8455 ± 90	s-pf	Tliapa	97 07.3′	19 03.6′	2
Upper	9006	8470 ± 160	pf	B. Escoba	97 22.4′	19 02.5′	4
Upper	PO-27	8580 ± 80	s-pf	Tliapa	97 07.3′	19 09.6′	This study
Upper	HV14367	8595 ± 85	s-pf	Teteltzingo	97 09′	19 03.5′	2
Upper	PA-46	8620 ± 140[b]	s&af	Tlacouatl	?	?	1
Upper	PO-133	8630 ± 90	s-pf	Teteltzingo	97 09′	19 09.5′	This study
Upper	PO-101C	8660 ± 80	s-pf	Loma Grande	97 14.9′	18 55.2′	This study
Lower	PO-133′	8690 ± 50	s-pf	Teteltzingo	97 08.8′	19 03.3′	This study
Lower	A74.2	8710 ± 70[b]	s&af	B. Tecajete	?	?	1
Lower	PO-101b′	8760 ± 70	s-pf	Loma Grande	97 14.9′	18 55.2′	This study
Lower	PO-93	8770 ± 90	s-pf	Xometla	97 09.6′	19 03.3′	5
Lower	PO-145	8860 ± 60	s-pf	Excola	97 08.2′	19 08.1′	This study
Lower	PO-78	8980 ± 80	s-pf	Maltrata	97 13.8′	18 48.8′	This study
Upper*	PU-146	9400 ± 170[c]	s&af	Teteltzingo	97 09′	10 09.5′	3
–	PU-141	10600 ± 190[d]	a.fall	Summit	?	?	3
–	PU-111	12900 ± 150	s&af	Chocaman	?	?	3
–	PO-89	13270 ± 90	s&af	Chocaman	97 02.4′	19 01.5′	5

Key: Deposit: p.fall = pumice fall, r.af = reworked ash flow, a.fall = ash airfall, b&af = block-and-ash flow, s&af = scoria-and-ash flow, r.b&af = reworked block-and-ash flow, pf = pyroclastic flow, s-pf = scoria-pumice flow.
Reference: 1 = Höskuldsson and Robin (1993), 2 = Heine (written commun., 1992), 3 = Cantagrel et al. (1984), 4 = Siebe et al. (1993), and 5 = Carrasco-Núñez et al. (1993). * Dates compared in Table 4. See text for discussion.
Eruptive episodes proposed by Höskuldsson and Robin (1993): a = 'Loma Grande', b = 'Xilomich', c = 'Coscomatepec', d = 'Tlachichuca'.

not averaged. The difference in age between the upper and lower member is statistically highly significant. Although they are about 300 years apart, we judge that the two members, based on lithological and distributional similarities, can be considered part of the same eruptive episode.

The new radiometric dates include 3 resampled sites (#27, 133, 101; Fig. 2) that were reported by Cantagrel et al. (1984), whose data differed markedly from the range of 8500 to 9000 yr. B.P. We attempted to sample the identical sites as described by those authors and these were also resampled and reanalyzed in 2 cases by K. Heine (written commun., 1992). The new data, a total of 5 new ^{14}C dates are compared with previous reported dates in Table 4. We could not duplicate any of the disparate ages originally reported by Cantagrel et al. (1984), and instead found 5 dates that are within the 8500–9000 yr. B.P. range (Table 4).

The results in Table 4 do not support interpretations of Höskuldsson and Robin (1993) who, based on the data of Cantagrel et al. (1984), suggested that there were eruptive episodes called 'Loma Grande' and 'Coscomatepec' corresponding to about 6200 to 7020 yr. B.P., and 9400 yr. B.P. respectively (Table 3). Since these dates cannot be reproduced and samples from those sites are instead found to correspond to the age of the Citlaltépetl ignimbrite, we suggest that the Coscomatepec episode may not exist, and the Loma Grande episode should be reduced to a discrete and entirely different event that produced a single block-and-ash flow deposit at a different locality dated independently at 6640 ± 240 yr. B.P. by Höskuldsson and Robin (1993) (Table 3). They reported another 'block-and-ash-flow deposit' dated at 8170 ± 70 yr. B.P., which along with three other 'scoria-and-ash-flow deposits' dated at 8300 ± 70, 8620 ± 140, and 8710 ± 70 yr. B.P. form the 'Xilomich' eruptive episode of Höskuldsson and Robin (1993) (Table 3). These block-and-ash-flow deposits represent smaller scale events that are unrelated to the Citlaltépetl ignimbrite. According to field descriptions, the 8300 yr. B.P. deposit of Höskuldsson and Robin is similar to a pyroclastic flow dated at 8470 ± 160 yr. B.P. by Siebe et al. (1993), implying that the former deposit could correspond to the same episode that formed the Citlaltépetl ignimbrite. The dates of the Xilomich episode of Höskuldsson and Robin otherwise do fall in the 8500–9000 yr. range and also support our interpretation of one large episode.

Höskuldsson and Robin (1993) described a Plinian pumice-fall layer (called 'T-II') on top of the 'Xilomich' sequence separating it from the scoria flows of their 'Loma Grande' episode. These scoria flows, in our interpretation (Table 4), correspond to the Upper member of the Citlaltépetl ignimbrite and the pumice-fall layer represent its basal part. The composition of both the pumice layer and the overriding pyroclastic flows is quite similar and the contact between them shows no sign of erosion. Furthermore, ^{14}C dates above and bellow the pumice-fall layer (as depicted in sections Loma Grande and Teteltzingo, Fig. 4d and 4f) demonstrate that all of these deposits could correspond to a single eruptive episode.

Table 4
Comparison of ^{14}C dates (years B.P.) for pyroclastic-flow deposits at similar localities around Citlaltépetl volcano

Sample	Locality*	Cantagrel et al. (1984)	Heine, written commun.	This paper
101c	Loma Grande	6200 ± 120	–	8660 ± 80
27	Tliapa	7020 ± 120	8455 ± 90	8580 ± 80
133	Teteltzingo	9400 ± 170	8595 ± 85	8630 ± 90

8. Flow characteristics

The distribution of the studied deposits shows that the pyroclastic flows were topographically controlled and channeled through valleys and barrancas on the lower slopes of the volcano. We found no veneer deposits, which would provide evidence that the pyroclastic flows climbed topographic barriers.

The *aspect ratio* was defined by Walker et al. (1980) as the average flow thickness of the deposit divided by the diameter of a circle covering the same areal extent as the deposit. Using the areal extent of the deposits as preserved (mainly valley fills) the Citlaltépetl ignim-

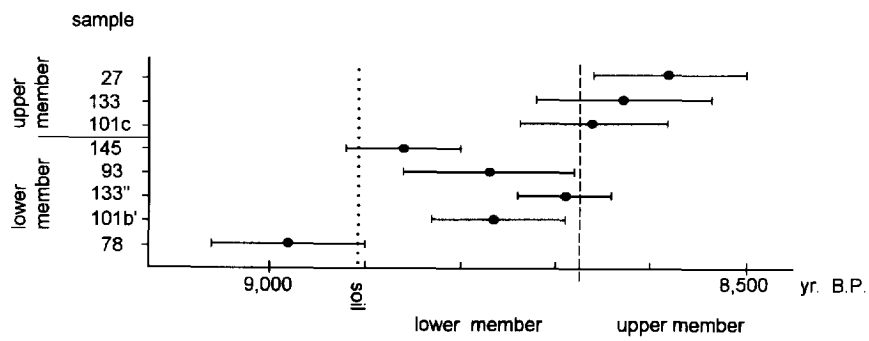

Fig. 11. Radiocarbon dates for the Citlaltépetl ignimbrite at different localities around the volcano and at distinct stratigraphic levels.

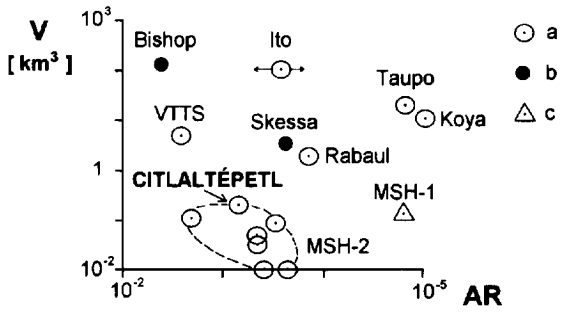

Fig. 12. Diagram of volume (V) against aspect ratio (AR: average thickness/diameter of a circle covering the same area as the deposit) for different types of ignimbrite and related deposits (after Walker, 1983). a = mainly non-welded; b = mainly welded; c = relatively poor in pumice; $VTTS$ = Valley of Ten Thousand Smokes; MSH = Mount St. Helens (1 = "directed blast" of May 18, 1980, 2 = post-climatic 1980 flows, which are grouped in the dashed area). Arrows for Ito ignimbrite express uncertainty.

brite has a low-to-intermediate *aspect ratio* 1:5000. It is volumetrically similar to those ignimbrites associated with the 1980 eruption of Mount St. Helens (Fig. 12). According to Wilson and Walker, (1981) a low to intermediate aspect ratio implies low-to-moderate flow velocities, and little eruptive violence. However, suggestions of violence comes from particular depositional structures observed (Fig. 4). These features include:

(a) *the basal layer of the Upper member* (Excola). This is a fines-depleted, pumice-rich layer similar to the ground layer observed in the Taupo ignimbrite, which was interpreted as the result of a strong air ingestion in the head of a high-velocity flow that produced intense segregation of pumice clasts.

(b) *the basal contact and the lee-side lenses at the lowermost flow in the Lower member* (Maltrata). The conspicuous, abrupt, and undulating contact between the basal layer of the Lower member's lowermost flow and the lee-side pumice lenses are also features of the Taupo ignimbrite (Wilson and Walker, 1981).

(c) *the grading and the segregated lenses in the Lower member* (Vaquería). The coarse-tail grading of large pumices towards top (reverse) and larger lithics towards base (normal), and the pumice and lithic lenses observed in proximal facies (<13 km from vent) in the Lower member are characteristics that can be caused by a relatively expanded flow produced under intermediate degrees of fluidization according to Wilson (1980).The absence of these structures downstream suggests a decreasing fluidization with distance.

9. Interpretations on the Citlaltépetl ignimbrite eruptions

The Citlaltépetl ignimbrites could have been generated by a process analogous to a low-pressure 'boiling-over' of gas-charged magma from an open vent such as was observed in the 1980 eruption of Mount St. Helens (Rowley et al., 1981) or reported in several other historical, small-volume eruptions (i.e. Mount Lamington, Papua in 1951, Taylor, 1958; Cotopaxi, Ecuador, Wolf, 1878). In support of this we note that the Citlaltépetl ignimbrite: (a) contains a dominant proportion of nonvesiculated, high-density scoriaceous clasts that may reflect the instantaneous collapse of the extruded material, without formation of a convective column; (b) has a relatively small volume (~ 0.25 km^3); (c) is not associated with thick sequences of Plinian fall deposits; and (d) does not contain samples of basement rocks (limestone and shale) found at about 3 km depth, which suggests an apparently shallow reservoir.

Magma mixing is proposed as the triggering mechanism (Sparks et al., 1977) that produced the explosive eruption of scoria-flows at Citlaltépetl. We suggest that a sudden intrusion of a nonvesiculated, but gas-rich andesitic magma into a differentiated, shallow-level, dacitic reservoir occurred. This could have produced superheating, induced convection, and increased pressure in the dacitic magma, resulting in fracture of the wall rocks. Dacitic magma supersaturated in a volatile phase would then undergo sudden decompression producing strong vesiculation and exsolution of gases, which are responsible in part for the mobility of the pyroclastic flows. Vesiculation of the scoria particles could be inhibited in the presence of groundwater, which may favor rapid quenching to form glassy textures. The magma probably ascended rapidly, so that the granodioritic fragments of the reservoir walls were incorporated without signs of melting (granodioritic inclusions within scoria fragments). Mixing was inhibited in most cases, forming andesitic and dacitic end-member pumices; banded and mixed pumice indicate incomplete or partial mixing.

The distribution of the deposits, with preferential abundance of multiple flow units at proximal facies (<13 km from vent) and single units at distal areas (southern flank), and internal structures of flows (such as segregated lenses and grading) suggest a significant

variation in the intensity of the eruptions that produced the young Citlaltépetl scoria and pumice flows. Initial eruptions were apparently very energetic (wider distribution) and intensity generally declined with time.

10. Implications for hazard assessment

Table 3 lists most of the known ^{14}C ages for volcanic deposits at Citlaltépelt, a list that includes all of the ages discussed in this paper. Analysis of the dates shown in Table 3 reveals the existence of three main explosive eruptions that occurred 13,000, 8500–9000 (Citlaltépetl Ignimbrite, the subject of this paper) and 4000–4600 years ago. The 13,000 yr. B.P. eruption is supported by two radiocarbon dates: at $12,900 \pm 150$ yr. B.P. (Cantagrel et al., 1984), and at $13,270 \pm 90$ yr. B.P. (this study). It formed a directed pumice flow that was emplaced on the volcano's eastern flank (Chocaman, see Fig. 2). The overall composition of this deposit is dacitic, similar to that of the Citlaltépetl Ignimbrite but it lacks scoria fragments. In addition, about 4000 to 4600 yr. B.P., an important co-eruptive event simultaneously produced several block-and-ash flow deposits and other associated volcaniclastic deposits at different locations around Citlaltépetl Volcano. On the western flank, this eruptive phase produced a fan-shaped deposit consisting of a complex association of block-and-ash flow, pyroclastic-flow, and laharic deposits (Siebe et al., 1991, 1993), which were apparently related to the emplacement of a dacitic dome at the summit crater. Similar block-and-ash flow deposits are also found at the southwest lower slopes of Citlaltépetl indicating a much bigger eruptive episode (Carrasco-Núñez, 1993).

A large eruptive volume peak is proposed by Höskuldsson and Robin (1993) at about 10,600 yr. B.P. However, the estimated volume for that eruptive period corresponds to a lava flow that is apparently covered by pyroclastic deposits from the 'Coscomatepec' episode (9400 yr. B.P. according to Cantagrel et al., 1984; and 8630 yr. B.P. according to this paper). For that reason, Höskuldsson and Robin (1993) suggested that the lava flow belonged to an episode called 'Tlachichuca' about 10,600 yr. B.P. The only age constraint is that the lava flow is older than 8630 years, but it could be much older than 10,600 years. Furthermore, these authors described two pyroclastic-flow deposits at La Perla locality, whose volume could not be estimated, that were included in the Tlachichuca episode even though there was no stratigraphic relationship with the tephra layer that Robin and Cantagrel (1982) dated at 10,600 yr. B.P. (this date was obtained from a deposit at a different location in the NE summit area of Citlaltépetl). In summary, evidence for a voluminous eruptive peak at 10,600 yr. B.P. is weak, in our opinion.

During the last 4000–5000 years the volcano has erupted mainly dacitic lavas (Carrasco-Núñez, 1993). Historical records indicate mild activity with only spo-

Table 5
Historic activity at Citlaltépetl Volcano (Pico de Orizaba)

Date	Description	Reference
1974	Relative warming of soil around the crater	Crausaz (1994)
1920–1921	Debris flows and steam escaping from the summit area	Crausaz (1994)
1830–1866	Fumarolic activity	Crausaz (1994)
1687	Ash eruption	Mooser et al. (1958)
1630	There was not eruption (misprint in Mooser et al. (1958)	Crausaz (1994)
1613	Unconfirmed activity	Waitz (1910)
1569–1589	Ash eruptions	Crausaz (1994)
1566	Lava flows from central crater	Waitz (1910), Mooser et al. (1958)
1559	Unconfirmed activity	Crausaz (1994)
1545	Ash and lava flows from central crater	Waitz (1910), Mooser et al. (1958)
1533–1539	Ash eruptions	Crausaz (1994)
1351	Unconfirmed activity	Crausaz (1994)
1264–1265	Unconfirmed activity	Crausaz (1994)
1187	Unconfirmed activity	Crausaz (1994)
1157	Unconfirmed activity	Crausaz (1994)

radic eruptions of viscous dacitic lava flows and minor ash eruptions (Table 5). This summary of Citlaltépetl's recent eruptive behavior indicates that although the eruptive pattern is noncyclical and diverse, major pyroclastic eruptions appear to recur at intervals of roughly 4000 years and follow long repose periods.

There is a common denominator in all recent eruptions at Citlaltépetl. The overall composition of most volcanic products is comparatively similar for both pyroclastic and lava materials (Fig. 8). This implies that if the lavas that form the present cone are the product of long periods of magma homogenization (Carrasco-Núñez, 1993) they possibly result from the replenishment of a silicic magma reservoir by a juvenile basaltic-andesitic magma. This replenishment may be a periodic process that, in some cases, may trigger explosive eruptions. Thus it is possible that an explosive eruption could occur in the future considering that the last major pyroclastic-flow-forming eruption occurred 4000 years ago. Citlaltépetl is characterized by long periods of repose that are comparable to other stratovolcanoes such as Mount Pinatubo (Pinatubo Volcano Observatory Team, 1991) or Santa María (Williams and Self, 1983), which explosively resumed activity after reposes that lasted hundreds to thousands of years.

If renewed explosive activity at Citlaltépetl occurred, similar to the eruption of 8500–9000 yr. B.P., an area as large as 2500 km^2 could be devastated, including numerous settlements and economically important agricultural crops. Because of the asymmetrical topography on which Citlaltépetl grew, about 1200 m lower on the eastern slope than the western one, slope gradients to the east are much greater. Flows to the east would be channeled through river-valleys in contrast to the western sector, where they mainly would widen in an open-valley topography, and thus H/L (ratio of vertical elevation difference and horizontal transport distance; Siebert, 1984) values are 0.17 to the east, and 0.21 to the west. Furthermore, the volcanic risk is greater to the east because an important settlement (Orizaba city) is located in the direct path of possible future flow-type events. Orizaba and nearby towns, with a population of about 175,000 inhabitants, are now resting on a thick pile of volcaniclastic deposits including the 8500–9000 yr. B.P. Citlaltépetl ignimbrite (Fig. 2).

Many other towns and villages having a combined population of at least 100,000 inhabitants could also be impacted in some way either by pyroclastic flows, ash clouds, or lahars. The latter could be produced by melting of ice and snow of the summit during the passage of hot pyroclastic material, would be mainly funneled through the Jamapa, Cuopa or Tliapa rivers affecting only small villages.

11. Conclusions

(1) A major Holocene eruptive period occurred at Citlaltépetl Volcano about 8500–9000 yr. B.P. producing a succession of scoria and pumice flows (Citlaltépetl ignimbrite). All units are compositionally similar and apparently represent a single eruptive phase, which lasted a few hundred years.

(2) The distribution of correlated deposits on all flanks is consistent with a summit eruption. The flows were then channeled in valleys and barrancas affecting all flanks of the volcano, and deposited at distances up to 25 to 30 km from the summit vent.

(3) The deposits represent an intermediate-aspect ratio ignimbrite that flowed with moderate velocities. Although the flows did not surmount high obstacles and they were apparently emplaced without much violence, some features suggest an expanded flow behavior and local turbulence during emplacement.

(4) The eruption was possibly associated with a low-pressure 'boiling-over' mechanism of a gas-charged magma in an open system.

(5) The eruption was associated with (and possibly triggered by) partial or incomplete mixing of two different magmas: a silicic andesite (59% in silica), and a dacite (67% in silica). These magma types have also been involved in younger eruptions, suggesting that the conditions that led to a devastating ignimbrite are still present.

Acknowledgements

Field expenses and radiometric dates were paid by both a grant from the International Program Branch of National Science Foundation (NSF), U.S.A., and the project IN103094 supported by D.G.A.P.A. (U.N.A.M., México). Logistical support was provided

by Instituto de Geología (U.N.A.M., México). During the preparation of this manuscript the first author (GCN) received a grant provided by the Consejo Nacional de Ciencia y Tecnología (CONACYT) through the 'Fondo para retener y repatriar a los investigadores mexicanos'. We want to thank Jose Luis Macías, Ted Bornhorst, and Ciro Sandoval for reviewing an earlier draft of this manuscript. Comments and constructive criticism by Jim Luhr and Steve Nelson helped to improve this manuscript immeasurably.

References

Carrasco-Núñez, G., 1992. Estructura and estratigrafia de las lavas del Volcán Citlaltépetl, México. Second International Reunion on Volcanology, Colima, Mexico, Abstr., 82.

Carrasco-Núñez, G., 1993. Structure, eruptive history and some major hazardous events of Citlaltépetl volcano (Pico de Orizaba), México. Ph.D. dissertation, Michigan Technological University, U.S.A., 182 pp.

Carrasco-Núñez, G., Vallance, J.W. and Rose, W.I., 1993. A voluminous avalanche-induced lahar from Citlaltépetl volcano, México: Implications for hazard assessment. J. Volcanol. Geotherm. Res., 59: 35–46.

Cantagrel, J.M., Gourgaud, A. and Robin, C., 1984. Repetitive mixing events and Holocene pyroclastic activity at Pico of Orizaba and Popocatépetl (México). Bull. Volcanol., 47: 735–748.

Crausaz, W., 1986. A history of geological exploration in the Pico de Orizaba region, Mexico. Geol. Soc. Am., 99th annual meeting, abstr. with progr., 18: 574.

Crausaz, W., 1994. Pico de Orizaba or Citlaltépetl: Geology, archaeology, history, natural history and mountaineering routes. Geopress International, Ohio, U.S.A.

Dungan, M.A. and Rhodes, J.M., 1978. Residual glasses and melt inclusions in basalts from DSDP legs 45 and 46: Evidence for magma mixing. Contrib. Mineral. Petrol., 67: 417–431.

Eichelberger, J.D., 1978. Andesitic volcanism and crustal evolution. Nature, 275, 21–27.

Freundt, A. and Schmincke, H.U., 1985. Hierarchy of facies of pyroclastic flow deposits generated by Laacher See-type eruptions. Geology, 13: 278–281.

Halsor, S.P., 1989. Large glass inclusions in plagioclase phenocyrsts and their bearing on the origin of mixed andesitic lavas at Tolimán Volcano, Guatemala. Bull. Volcanol., 51: 271–280.

Hooper, P.R., 1964. Rapid analyses of rocks by X-ray fluorescence. Anal. Chem., 36: 1271–1276.

Hooper, P.R. and Atkins, L., 1969. The preparation of fused samples in X-ray fluorescence analyses. Mineral. Mag., 37: 409–413.

Höskuldsson, A., 1992. Le complexe volcanique Pico de Orizaba–Sierra Negra–Cerro Las Cumbres (Sud-Est Mexicain): Structure, dynamismes éruptifs et évaluations des areas. Ph.D. dissertation, University of Blaise Pascal, France, 210 pp.

Höskuldsson, A. and Robin, C., 1993. Late Pleistocene to Holocene eruptive activity of Pico de Orizaba, Eastern Mexico. Bull. Volcanol., 55: 571–587.

Le Bas, M.J., Le Maitre, R.W., Streckeisen, A. and Zanettin, B., 1986. A chemical classification of volcanic rocks based on the total alkali-silica diagram. J. Petrol., 27: 745–750.

Mooser, F., Meyer-Abich, H., McBirney, A.R., 1958. Catalogue of Active Volcanoes of the World: Part VI, Central America: Napoli, International Association of Volcanology, 146 pp.

Pinatubo Volcano Observatory Team, 1991. Lessons from a major eruption: Mt. Pinatubo, Philippines. EOS, Trans. Am. Geophys. Union, 73: 545–556.

Robin, C. and Cantagrel, J.M., 1982. Le Pico de Orizaba (Mexique). Structure et evolution d'un grand volcan andesitique complexe. Bull. Volcanol., 45: 299–315.

Robin, C., Cantagrel, J.M. and Vincent, P., 1983. Les nuées ardentes de type Saint-Vincent, épisodes remarquables de l'evolution récente du Pico de Orizaba (Mexique). Bull. Soc. Géol. France, 5: 727–736.

Rowley, P.D., Kuntz, M.A. and MacLeod, N.S., 1981. Pyroclastic flow deposits. In: P.W. Lipman and R.D. Mullineaux (Editors), The 1980 Eruptions of Mount St. Helens, Washington. U.S. Geol. Surv., Prof. Pap., 1250: 489–512.

Sheridan, M.F., Wohletz, K.H. and Dehn, J., 1987. Discrimination of grain-size subpopulations in pyroclastic deposits. Geology, 15: 367–370.

Siebe, C., Abrams, M. and Sheridan, M., 1991. Holocene age of a major block-and-ash-flow fan at the western slopes of Pico de Orizaba volcano. Primer Congreso Mexicano de Mineralogía, México, (abstracts), 203.

Siebe, C., Abrams, M. and Sheridan, M., 1993. Holocene block-and-ash flow fan at the W slope of ice-capped Pico de Orizaba Volcano, Mexico: Implications for future hazards. J. Volcanol. Geotherm. Res., 59: 1–31.

Siebert, L., 1984. Large volcanic debris avalanches—characteristics of source areas, deposits and associated eruptions. J. Volcanol. Geotherm. Res., 22: 163–197.

Sparks, R.S.J., Self, S. and Walker, G.P.L., 1973. Products of ignimbrite eruptions. Geology, 1: 115–118.

Sparks, R.S.J., Sigurdsson, H. and Wilson, L., 1977. Magma mixing: a mechanism for triggering acid explosive eruptions. Nature, 267: 315–318.

Taylor, G.A., 1958. The 1951 eruption of Mount Lamington, Papua. Aust. Bur. Miner. Resour., Geol. Geophys. Bull., 38: 1–117.

Tsuchiyama, A., 1985. Dissolution kinetics of plagioclase in the melt of the system diopside-albite-anorthite, and origin of dusty plagioclase in andesites. Contrib. Mineral. Petrol., 89, 1–16.

Waitz, P., 1910. Observaciones geológicas acerca del Pico de Orizaba. Bol. Soc. Geol. Mex., 7: 67–76.

Walker, G.P.L., 1971. Grain size characteristics of pyroclastic deposits. J. Geol., 79: 696–714.

Walker, G.P.L., 1983. Ignimbrite types and ignimbrite problems, J. Volcanol. Geotherm. Res., 17: 65–88.

Walker, G.P.L., Hemming, R.F. and Wilson, C.J.N., 1980. Low aspect ratio ignimbrites. Nature, 283: 286–287.

Williams, S.N. and Self, S., 1983. The October 1902 Plinian eruption of Santa María volcano, Guatemala. J. Volcanol. Geotherm. Res., 16: 33–56.

Wilson, C.J.N., 1980. The role of fluidization in the emplacement of pyroclastic rocks: an experimental approach. J. Volcanol. Geotherm. Res., 8: 231–249.

Wilson, C.J.N. and Walker, G.P.L., 1981. Violence in pyroclastic flow eruptions. In: S. Self and R.S.J. Sparks (Editors), Tephra Studies. D. Reidel, Dordrecht, 441–448.

Wilson, C.J.N. and Walker, G.P.L., 1982. Ignimbrite depositional facies: the anatomy of a pyroclastic flow. J. Geol. Soc. London, 139: 581–592.

Wright, J.V., Smith, A.L. and Self, S., 1980. A working terminology of pyroclastic deposits J. Volcanol. Geotherm. Res., 8: 315–336.

Wolf, T., 1878. Der Cotopaxi und seinletze eruption am 26 Juni, 1877. Neues. Jahrb. Mineral. Geol. Palantol., pp. 113–67.